29 p.

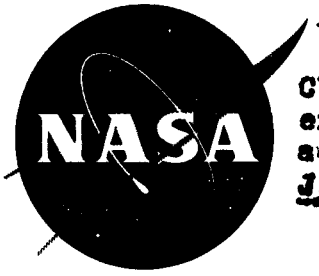

TECHNICAL MEMORANDUM

X-292

WIND-TUNNEL INVESTIGATION AT MACH NUMBERS FROM 0.50 TO 1.14 OF THE STATIC AERODYNAMIC CHARACTERISTICS OF A MODEL OF A PROJECT MERCURY CAPSULE

By Albin O. Pearson

Langley Research Center
Langley Field, Va.

NATIONAL AERONAUTICS AND SPACE ADMINISTRATION

WASHINGTON July 1960

NATIONAL AERONAUTICS AND SPACE ADMINISTRATION

TECHNICAL MEMORANDUM X-292

WIND-TUNNEL INVESTIGATION AT MACH NUMBERS FROM 0.50 TO 1.14 OF THE STATIC AERODYNAMIC CHARACTERISTICS OF A MODEL OF A PROJECT MERCURY CAPSULE*

By Albin O. Pearson

SUMMARY

The pitching-moment, normal-force, and axial-force characteristics of exit, reentry, and escape configurations of a 1/7-scale model of a Project Mercury capsule were investigated in the Langley 8-foot transonic pressure tunnel. The tests were conducted at angles of attack from approximately -2° to 85° for the exit and reentry configurations and from about -2° to 20° for the escape configuration. The Reynolds number varied from about 2.43×10^6 to 3.69×10^6.

The results show that all the model configurations trimmed at angles of attack near 0° and that the exit configuration was statically unstable; whereas the reentry and escape configurations had positive static stability. The addition of the tower and escape rocket to the exit configuration had a negligible effect on the slope of the normal-force coefficient but increased the axial-force coefficients.

INTRODUCTION

Results obtained from wind-tunnel investigations of models of blunt, nonlifting capsules which may be used as possible reentry vehicles (refs. 1 to 5) have aided in the development of a reentry capsule for use in Project Mercury. Additional wind-tunnel tests have been initiated by the National Aeronautics and Space Administration to determine the static aerodynamic characteristics of this capsule over large ranges of Mach number and angle of attack. The results of some of these tests at supersonic speeds are given in reference 6.

*Title, Unclassified.

The present investigation was performed in the Langley 8-foot transonic pressure tunnel and provides static aerodynamic data at subsonic and transonic speeds for a model similar to the capsule of reference 6. The model was tested as a reentry configuration (blunt end facing the relative wind), as an exit configuration (small cylindrical end facing the relative wind), and as an escape configuration (same as the exit configuration but with a tower and simulated rocket container attached to the cylindrical end). The investigation was performed at Mach numbers from about 0.50 to 1.14 and at angles of attack from approximately -2° to 85° for the exit and reentry configurations. The escape configuration was tested at angles of attack from about -2° to 20°. The Reynolds number, based on maximum body diameter, varied from about 2.43×10^6 to 3.69×10^6.

SYMBOLS

The data presented herein are referred to the body system of axes with the origin located at the model center-of-gravity position. The positive directions of forces, moments, and displacements are shown in figure 1. The coefficients and symbols are defined as follows:

C_m pitching-moment coefficient, $\frac{\text{Pitching moment}}{qAd}$

C_{m_α} slope of pitching-moment coefficient per degree at $\alpha \approx 0^\circ$, $\frac{\partial C_m}{\partial \alpha}$

C_N normal-force coefficient, $\frac{\text{Normal force}}{qA}$

C_{N_α} slope of normal-force coefficient per degree at $\alpha \approx 0^\circ$, $\frac{\partial C_N}{\partial \alpha}$

C_A axial-force coefficient, $\frac{\text{Axial force}}{qA}$

$C_{A,\alpha \approx 0}$ axial-force coefficient at $\alpha \approx 0^\circ$

$C_{p,c}$ model-balance chamber-pressure coefficient, $\frac{\text{Chamber pressure - Free-stream static pressure}}{q}$

M free-stream Mach number

q	free-stream dynamic pressure, lb/sq ft
R	Reynolds number based on maximum body diameter and free-stream conditions
d	maximum body diameter, 10.643 in.
r	radius, in.
A	maximum cross-sectional area, 0.6175 sq ft
α	angle of attack of model center line, deg

MODELS, TESTS, AND ACCURACY

Details of the 1/7-scale model configurations tested are shown in figure 2, and photographs are presented in figure 3. The capsule model used for the reentry configuration was a hollow body of revolution made from aluminum alloy. For this configuration the large, blunt end faced the relative wind. The exit configuration consisted of the same capsule model but had the small, cylindrical end facing the relative wind. The escape configuration was composed of a cylindrical aluminum-alloy body, simulating a rocket container, mounted on a tower made from three cross-braced steel rods attached to the nose of the exit configuration. The two lower rods of the tower were in a horizontal plane.

The models were mounted on a three-component internally located strain-gage balance which was sting supported. Several model-sting-support arrangements were used in order to maintain the model near the tunnel center line throughout the angle-of-attack range (fig. 3) and also to attempt to minimize the effects of sting interference. The various sting arrangements were constructed so that overlapping angles of attack could be obtained at angles of attack near 40° and 60°.

The tests were conducted in the Langley 8-foot transonic pressure tunnel at a stagnation pressure of 1.0 atmosphere and at a dewpoint temperature such that the air flow was free of condensation shocks. The variation of Reynolds number, based on maximum diameter, with Mach number is shown in figure 4. The model angle of attack, which was varied from about -2° to 85° for the exit and reentry configurations and from approximately -2° to 20° for the escape configuration, was determined by means of a calibrated, fixed-pendulum strain-gage unit located behind the model in the main sting support.

Normal force, axial force, and pitching moment were determined by means of the internal strain-gage balance with the pitching moments

referred to the center of gravity. The axial-force results are gross values and have not been adjusted to a condition of free-stream static pressure at the model base. Based upon balance accuracy and repeatability of data (neglecting any sting interference effects), it is estimated that the coefficients of normal force, axial force, and pitching moment are accurate within ±0.018, ±0.018, and ±0.004, respectively, at a Mach number of 0.50 and ±0.006, ±0.006, and ±0.001, respectively, at a Mach number of 1.14. The model-balance chamber-pressure coefficient $C_{p,c}$ was determined from the chamber pressure measured by an orifice inside the model in the strain-gage-balance chamber. All data presented from this investigation are essentially free from wall-reflected disturbances. The maximum variation of the actual test Mach numbers from the presented nominal values is less than ±0.005. Corrections were applied for tunnel flow angularity and for model sting and balance deflections. The accuracy of the angle of attack is estimated to be within ±0.20°.

RESULTS AND DISCUSSION

The pitching-moment, normal-force, and axial-force characteristics of the various configurations investigated are presented in figures 5 to 7 and are summarized in figure 8. At overlapping angles of attack near 40° and 60° (figs. 5 and 6), some interference effects due to sting-support arrangements are indicated. These effects are negligible on the pitching-moment and axial-force characteristics (figs. 5(a), 5(c), 6(a), and 6(c)) but are more pronounced on the normal-force characteristics (figs. 5(b) and 6(b), particularly for the exit configuration. The difference between the measured and faired values of C_N for the exit configuration amounts to a maximum of about 4 percent of the faired values at these larger angles of attack.

The variations of chamber-pressure coefficient with angle of attack are shown in figure 9.

Static Stability and Trim Characteristics

The exit configuration tested is statically unstable near angles of attack of 0°; whereas both the reentry and escape configurations have positive static stability. (See figs. 5(a), 6(a), 7(a), and 8.) The data of figures 5(a), 6(a), and 7(a) also show that the three configurations trim near an angle of attack of 0° and that a second, unstable trim point exists for the escape configuration near an angle of attack of 16°.

The model should be suitable for use as a reentry vehicle in that it meets the static stability and trim requirements stated in reference 1; that is, the capsule (without the tower and escape rocket) should trim and have positive static stability only when the heat sink (blunt face) faces the relative wind.

Normal- and Axial-Force Characteristics

The normal-force characteristics are shown in figures 5(b), 6(b), and 7(b) and are summarized in figure 8. For the reentry configuration, the values of C_{N_α} are negative throughout the Mach number range of this investigation. Addition of the tower and escape rocket to the exit configuration had little effect on C_{N_α}.

The axial-force coefficients for the reentry configuration (fig. 6(c)) are essentially constant with variation of angle of attack to about 20°. Addition of the tower and escape rocket to the exit configuration increased the axial-force coefficients. (See figs. 5(c) and 7(c).)

CONCLUDING REMARKS

The results of wind-tunnel tests of exit, reentry, and escape configurations of a reentry capsule, performed in the Langley 8-foot transonic pressure tunnel at Mach numbers from 0.50 to 1.14, indicate that the exit configuration trimmed near an angle of attack of 0° but was statically unstable. The reentry and escape configurations trimmed near an angle of attack of 0° but had positive static stability. The capsule, therefore, should be suitable for use as a reentry vehicle from a static-stability and trim viewpoint. The addition of the tower and escape rocket to the exit configuration had a negligible effect on the slope of the normal-force coefficient but increased the axial-force coefficients.

Langley Research Center,
National Aeronautics and Space Administration,
Langley Field, Va., March 3, 1960.

REFERENCES

1. Pearson, Albin O.: Wind-Tunnel Investigation at Mach Numbers From 0.40 to 1.14 of the Static Aerodynamic Characteristics of a Nonlifting Vehicle Suitable for Reentry. NASA MEMO 4-13-59L, 1959.

2. Turner, Kenneth L., and Shaw, David S.: Wind-Tunnel Investigation at Mach Numbers From 1.60 to 4.50 of the Static-Stability Characteristics of Two Nonlifting Vehicles Suitable for Reentry. NASA MEMO 3-2-59L, 1959.

3. Pearson, Albin O.: Wind-Tunnel Investigation at Mach Numbers From 0.20 to 1.17 of the Static Aerodynamic Characteristics of a Possible Reentry Capsule. NASA TM X-262, 1960.

4. Shaw, David S., and Turner, Kenneth L.: Wind-Tunnel Investigation of Static Aerodynamic Characteristics of a 1/9-Scale Model of a Possible Reentry Capsule at Mach Numbers From 2.29 to 4.65. NASA TM X-233, 1959.

5. Carter, Howard S., Kolenkiewicz, Ronald, and English, Roland D.: Principal Results From Wind-Tunnel Stability Tests of Several Proposed Space Capsule Models up to an Angle of Attack of 33°. NASA TM X-21, 1959.

6. Shaw, David S., and Turner, Kenneth L.: Wind-Tunnel Investigation of Static Aerodynamic Characteristics of a 1/9-Scale Model of a Project Mercury Capsule at Mach Numbers From 1.60 to 4.65. NASA TM X-291, 1960.

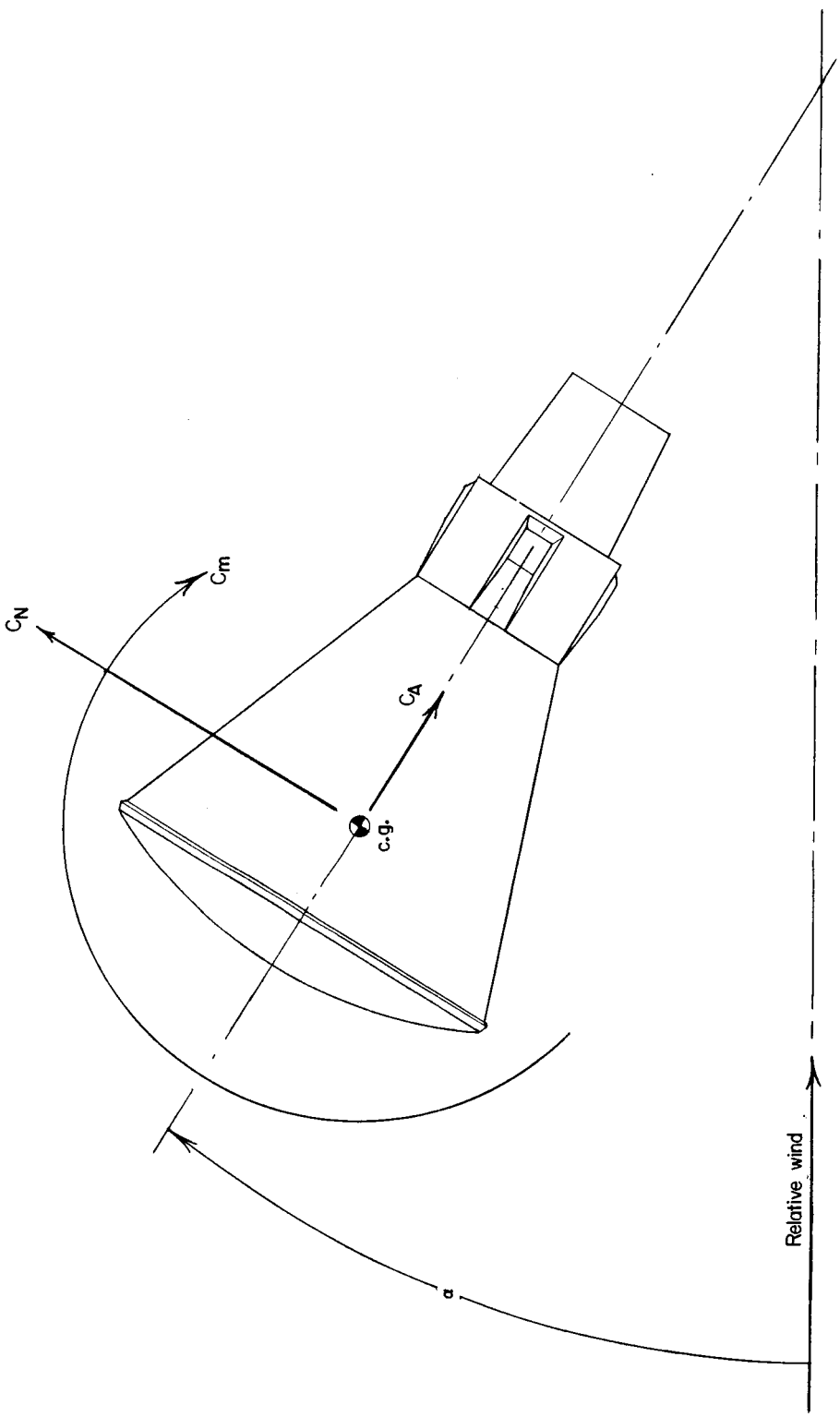

Figure 1.- Body axis system (reentry configuration shown). Arrows indicate positive direction.

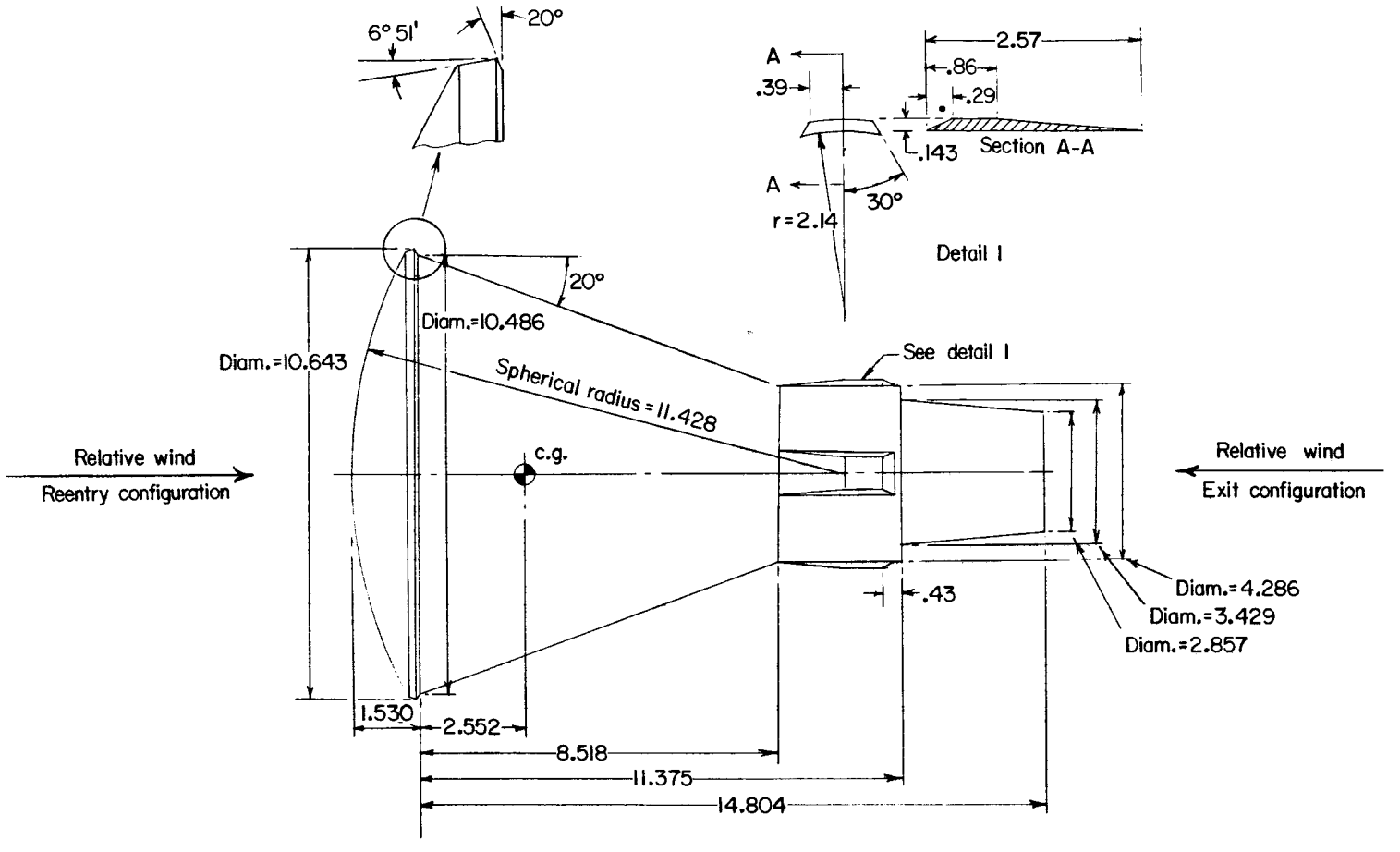

(a) Exit and reentry configurations.

Figure 2.- Details of model configurations. All dimensions are in inches unless otherwise noted.

CONFIDENTIAL

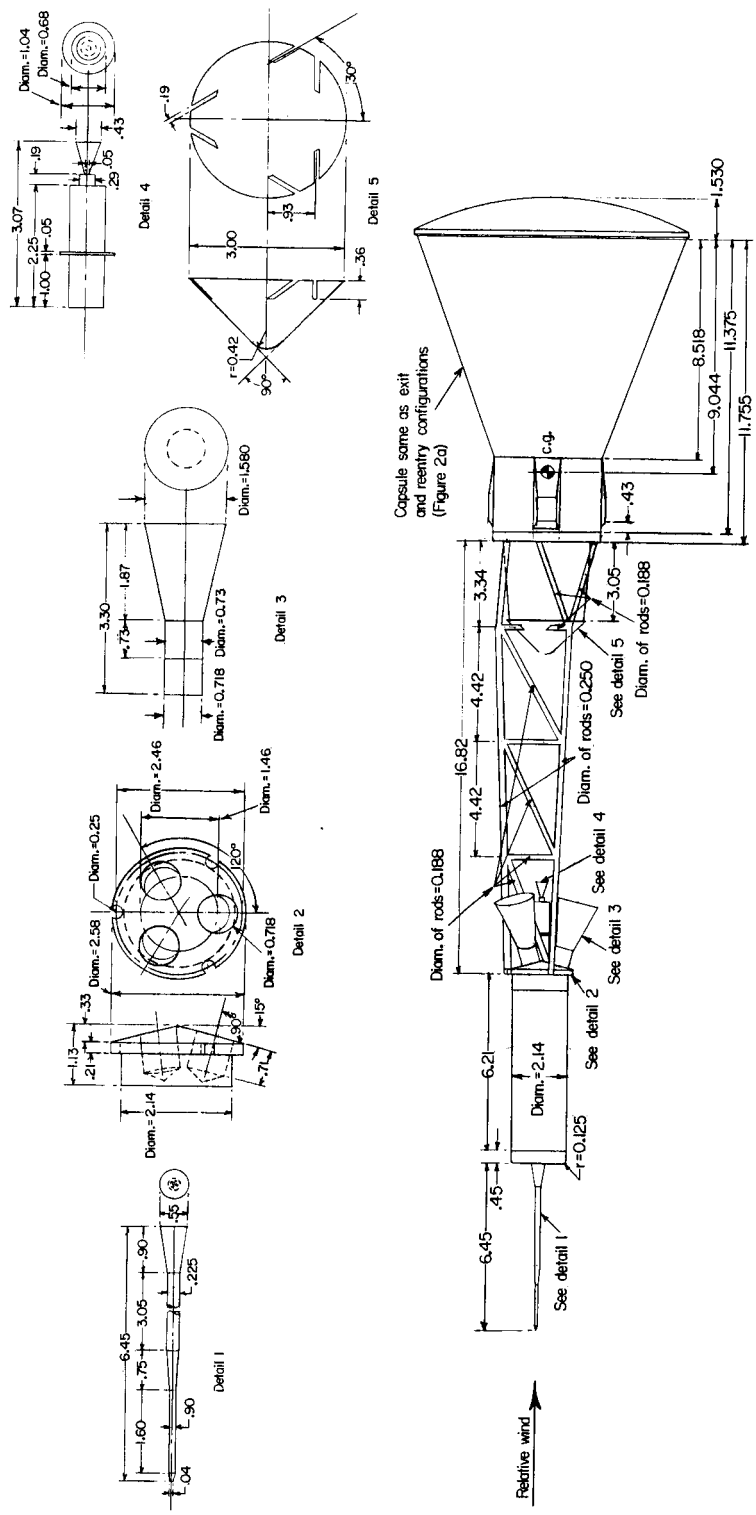

(b) Escape configuration.

Figure 2.- Concluded.

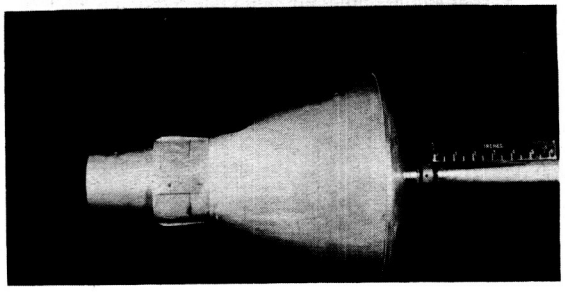

$\alpha \approx -2^{\circ}$ to 40°

L-59-7480

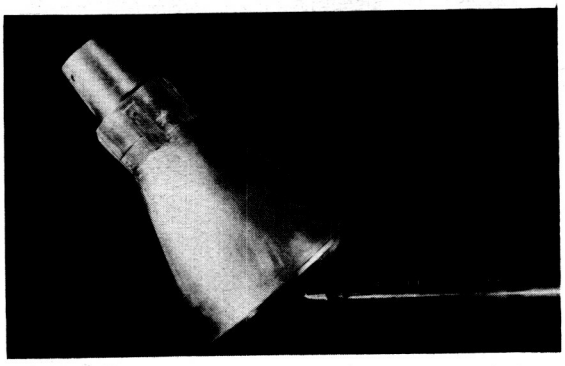

$\alpha \approx 40^{\circ}$ to 60°

L-59-7483

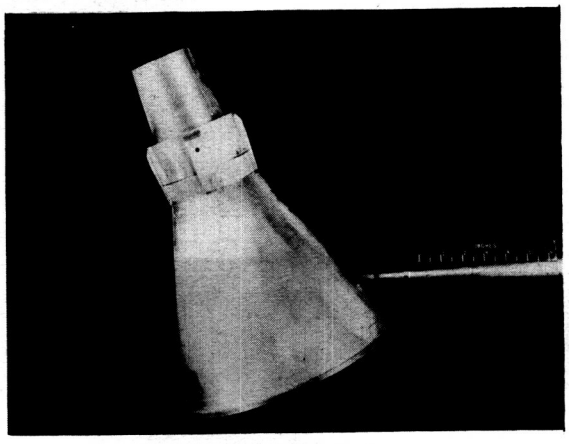

$\alpha \approx 60^{\circ}$ to 85°

(a) Exit configuration. L-59-7485

Figure 3.- Model configurations and sting-support arrangements.

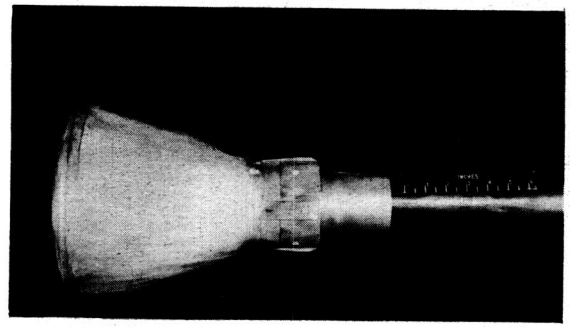

$\alpha \approx -2^{\circ}$ to 40°

L-59-7481

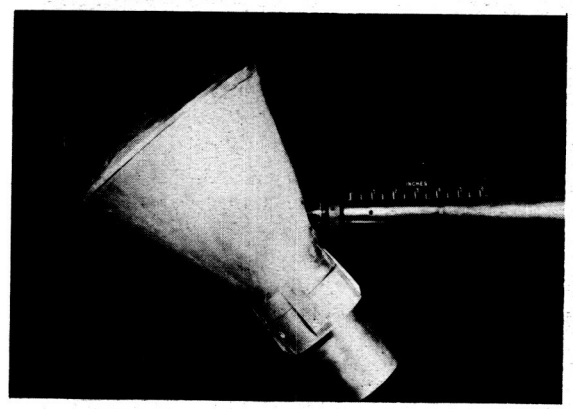

$\alpha \approx 40^{\circ}$ to 60°

L-59-7487

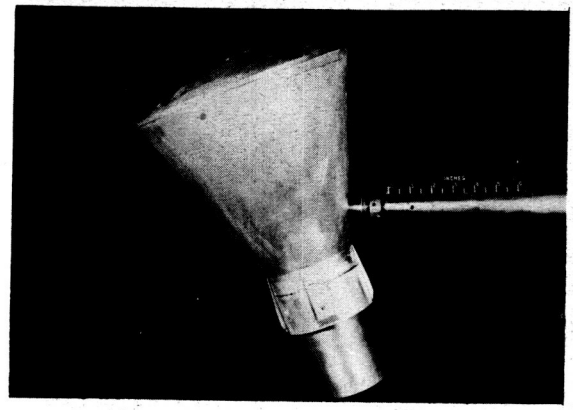

$\alpha \approx 60^{\circ}$ to 85°

(b) Reentry configuration. L-59-7486

Figure 3.- Continued.

$\alpha \approx -2^{\circ}$ to 20°

(c) Escape configuration. L-59-7478

Figure 3.- Concluded.

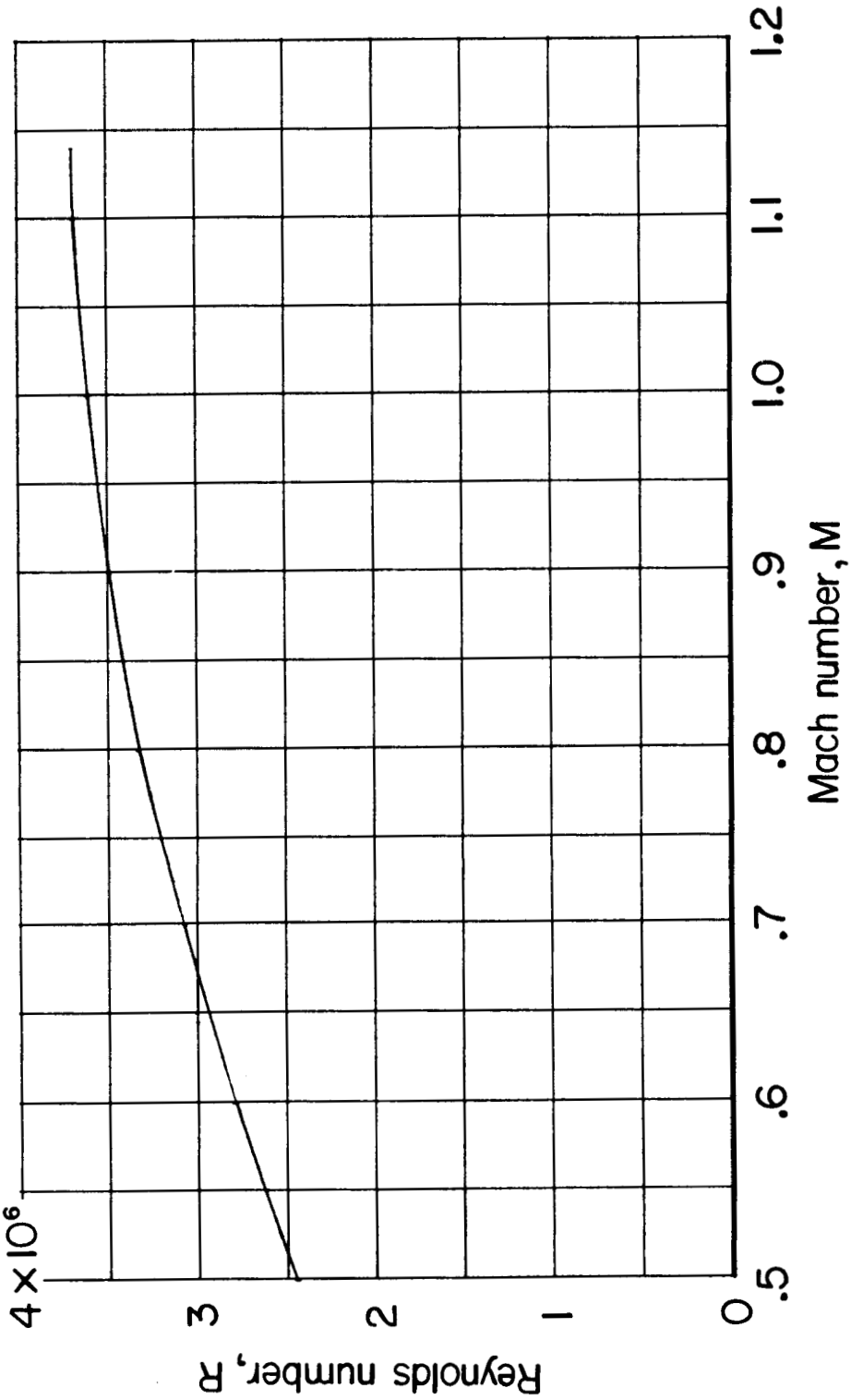

Figure 4.- Variation of test Reynolds number, based on maximum body diameter, with Mach number.

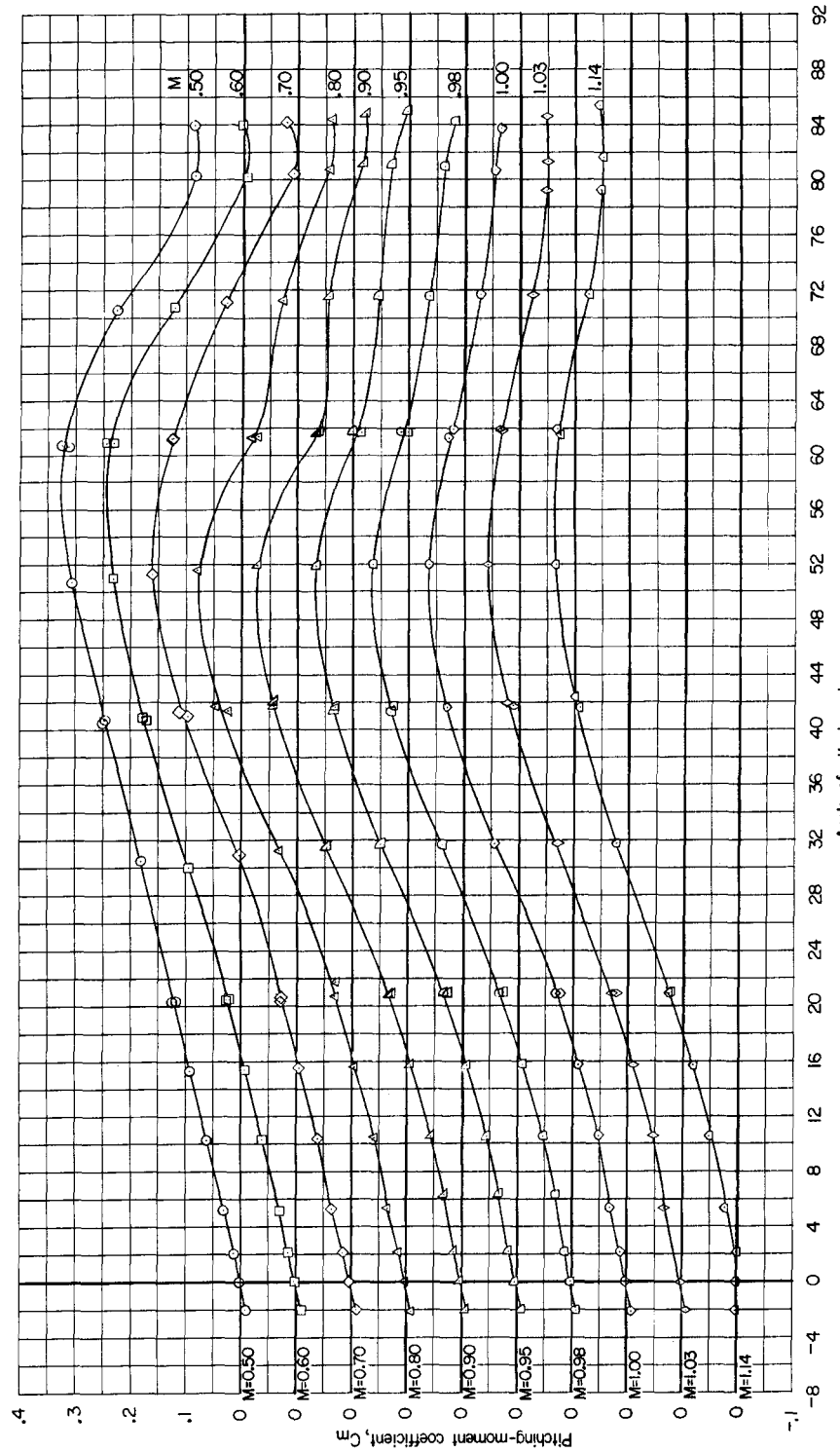

(a) Variation of C_m with α.

Figure 5.- Static aerodynamic characteristics of model in pitch. Exit configuration.

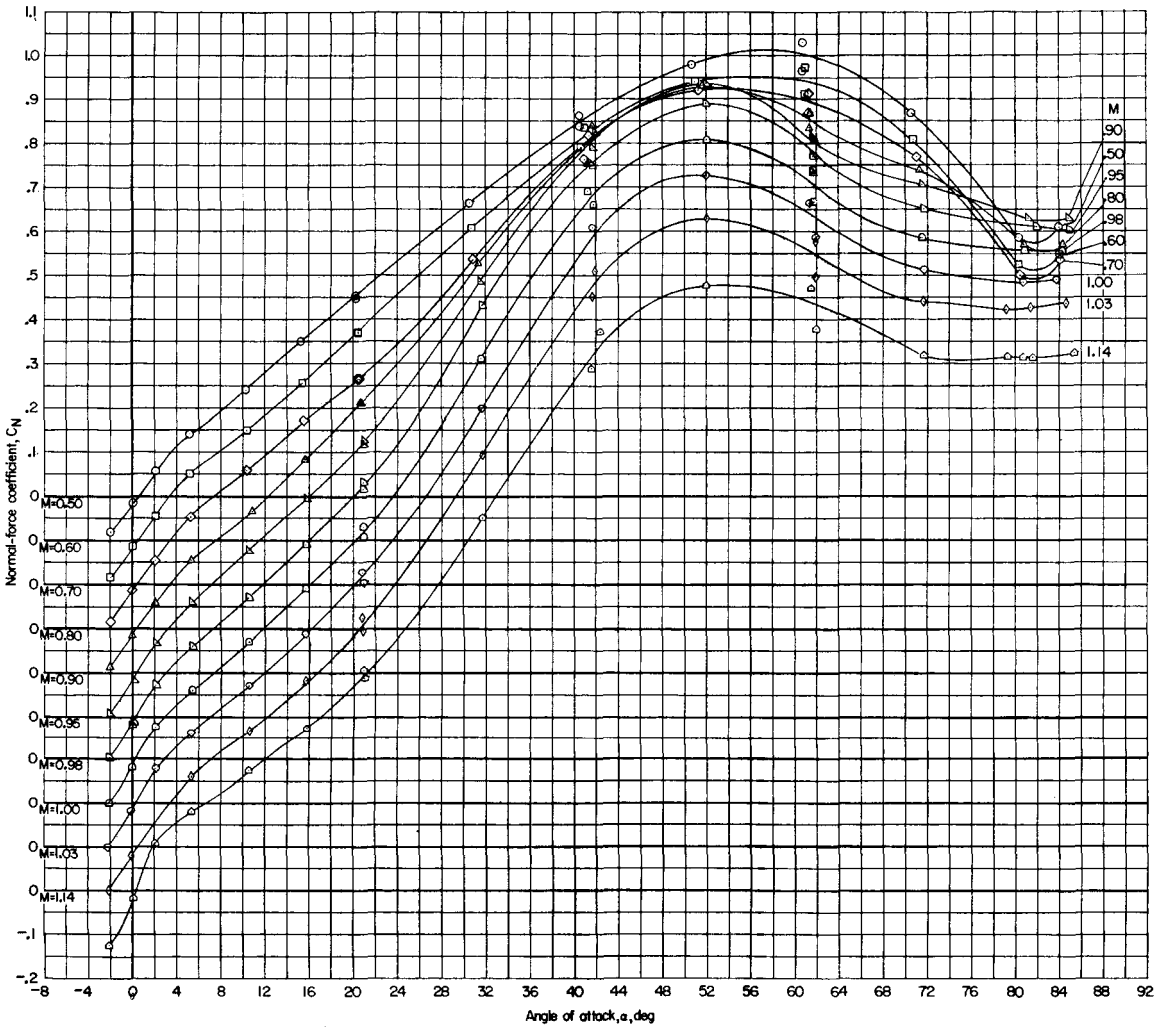

(b) Variation of C_N with α.

Figure 5.- Continued.

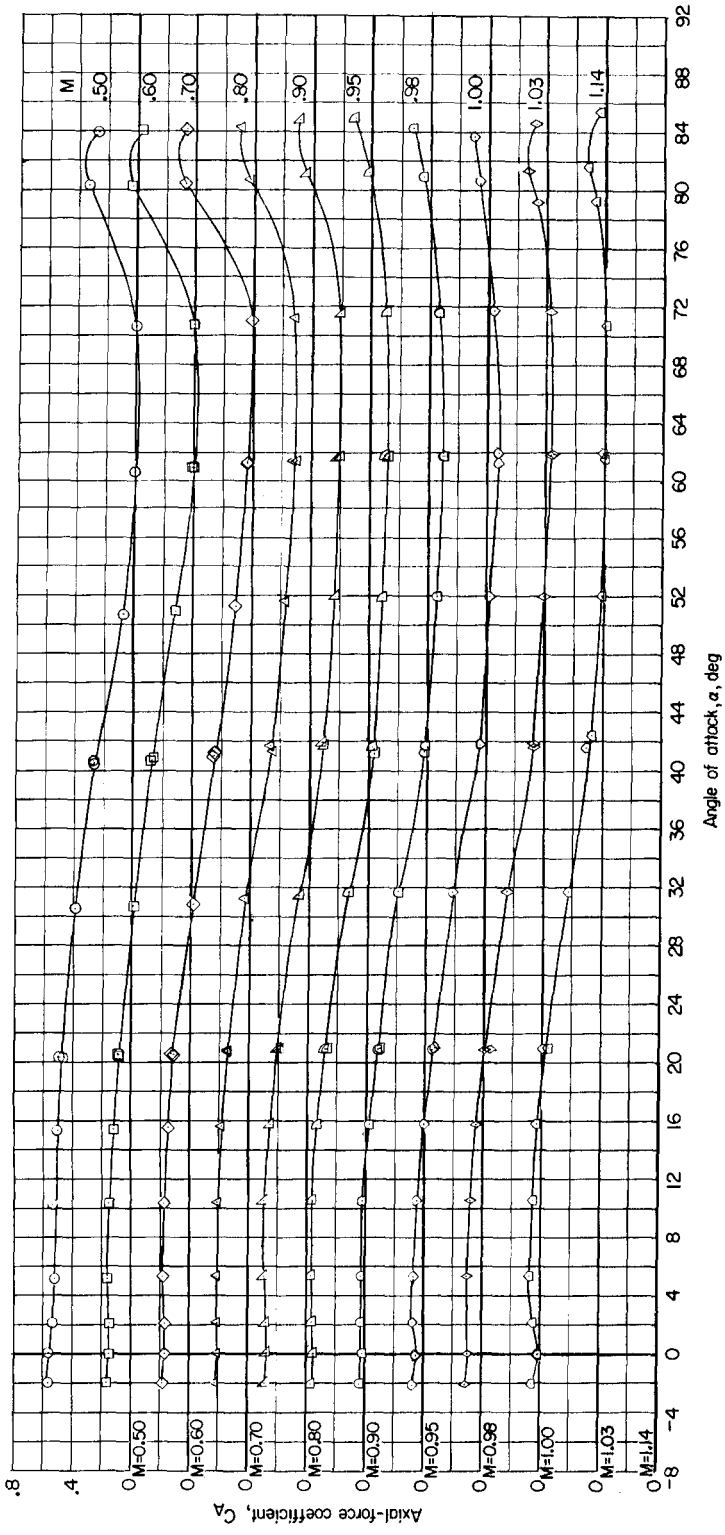

(c) Variation of C_A with α.

Figure 5.- Concluded.

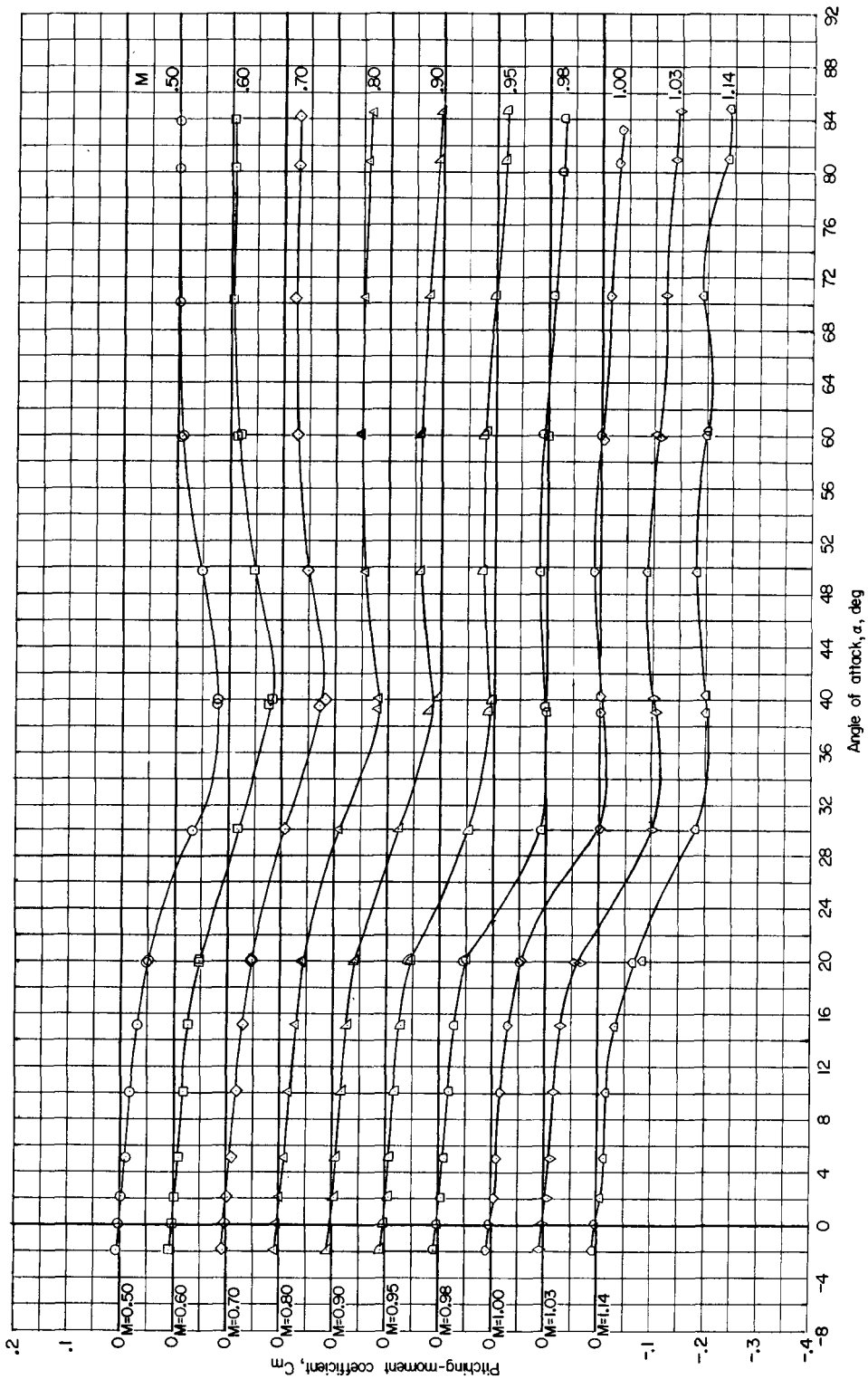

(a) Variation of C_m with α.

Figure 6.- Static aerodynamic characteristics of model in pitch. Reentry configuration.

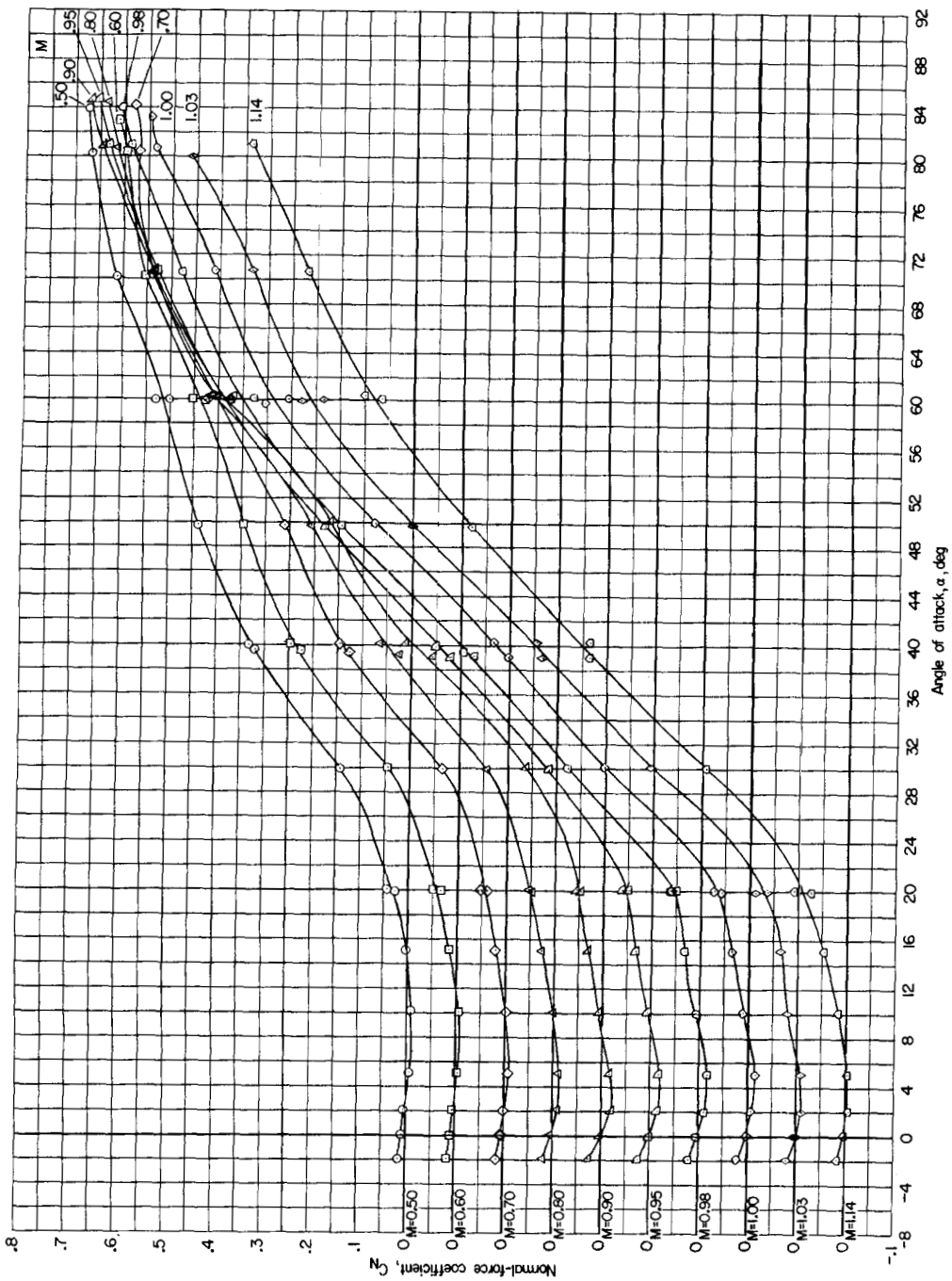

(b) Variation of C_N with α.

Figure 6.- Continued.

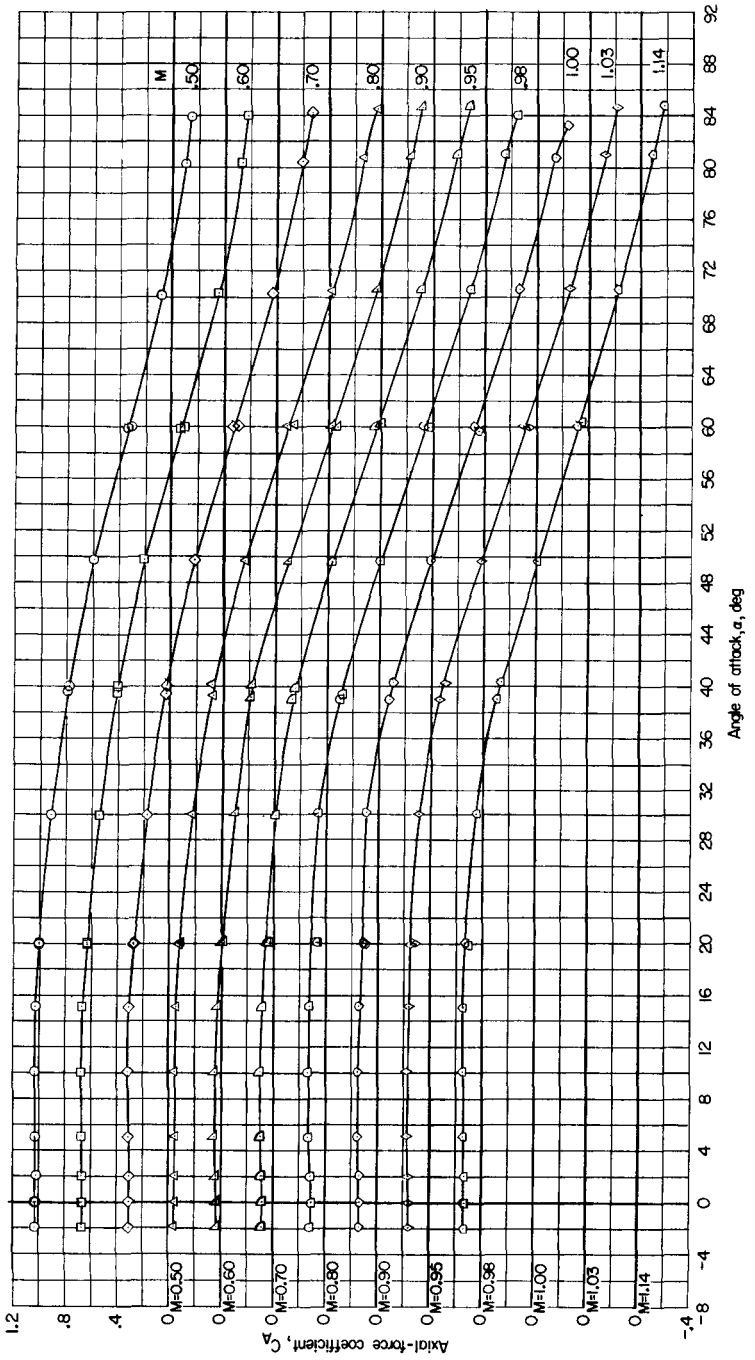

(c) Variation of C_A with α.

Figure 6.- Concluded.

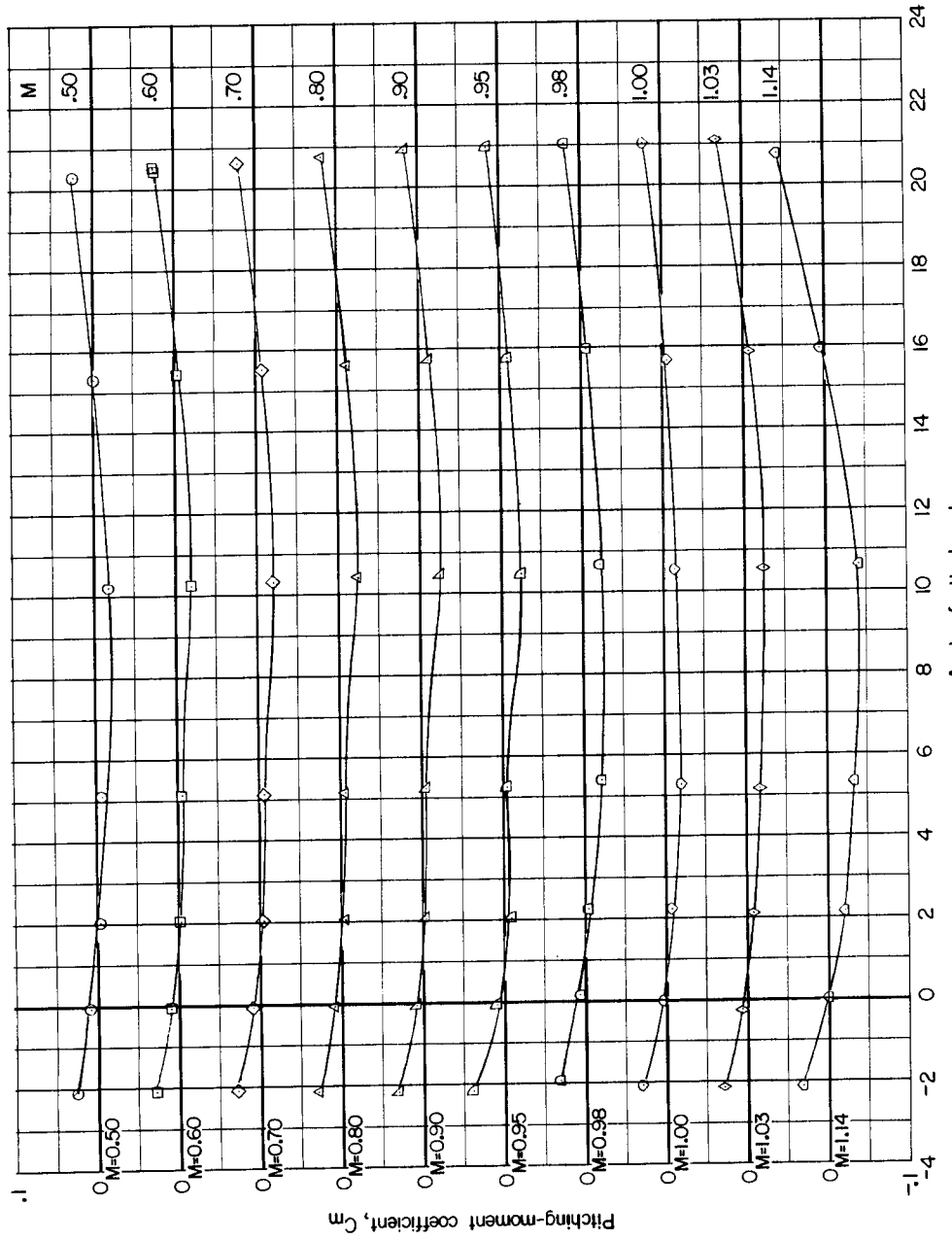

(a) Variation of C_m with α.

Figure 7.- Static aerodynamic characteristics of model in pitch. Escape configuration.

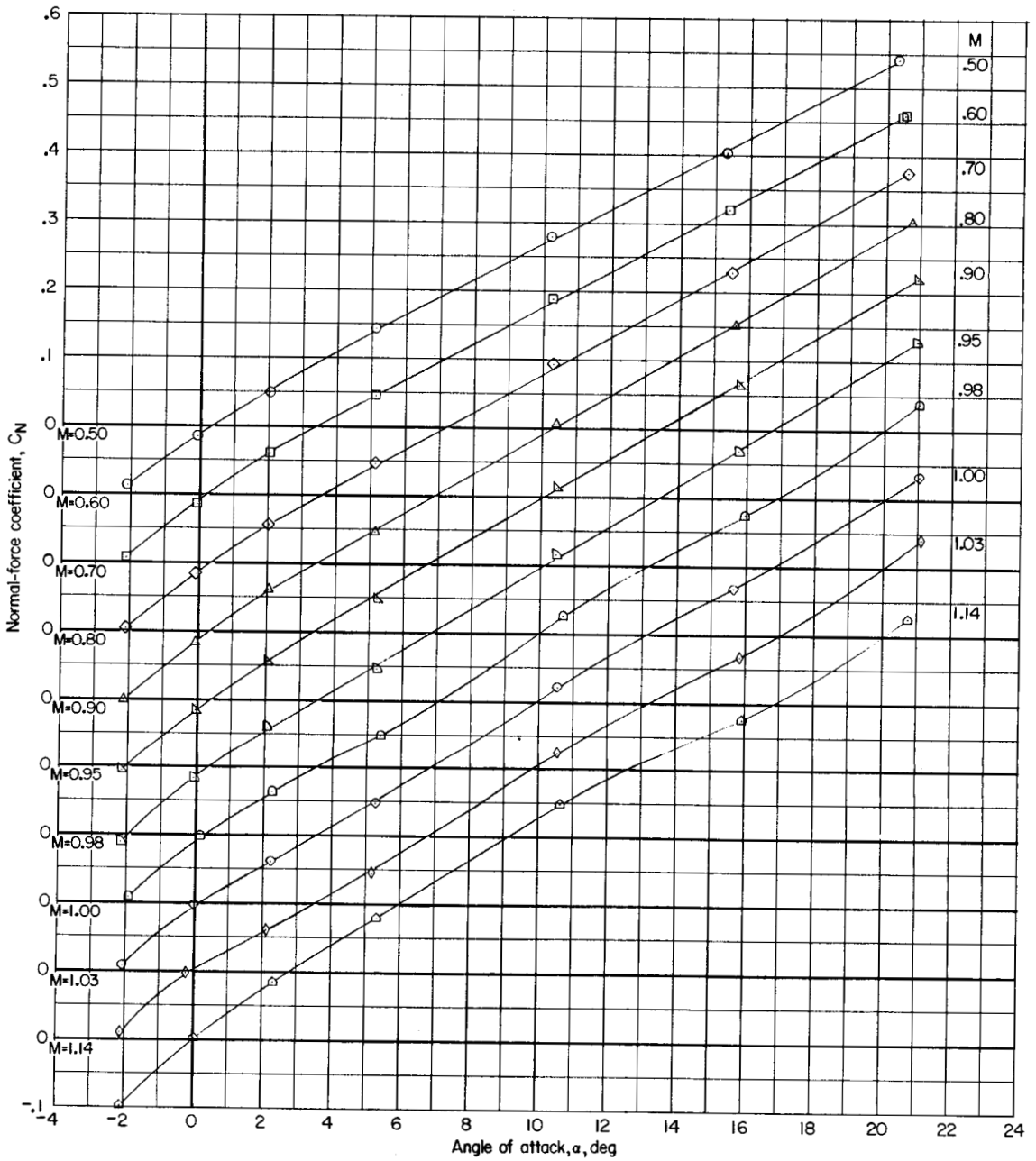

(b) Variation of C_N with α.

Figure 7.- Continued.

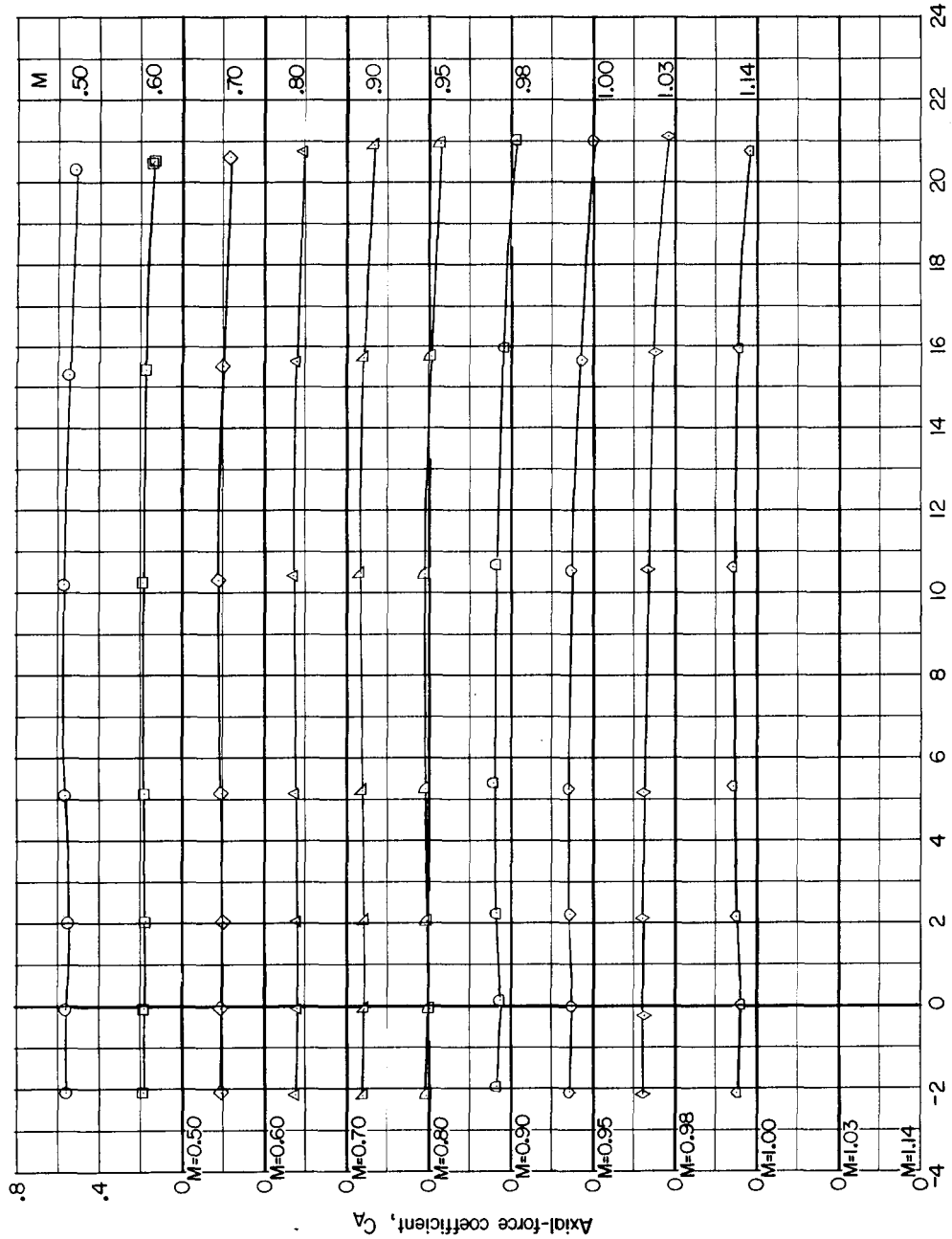

(c) Variation of C_A with α.

Figure 7.- Concluded.

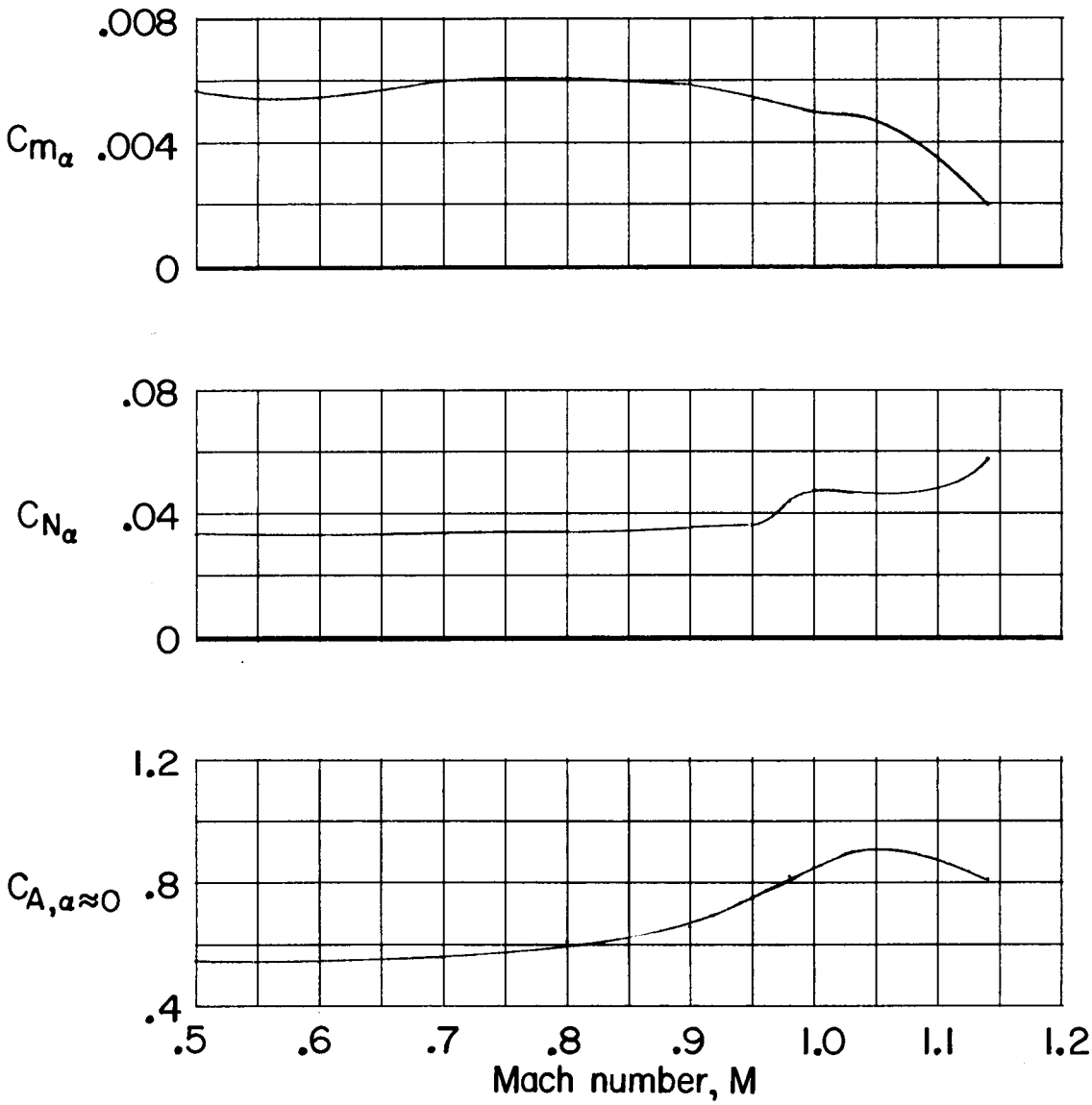

(a) Exit configuration.

Figure 8.- Summary of static aerodynamic characteristics of model in pitch.

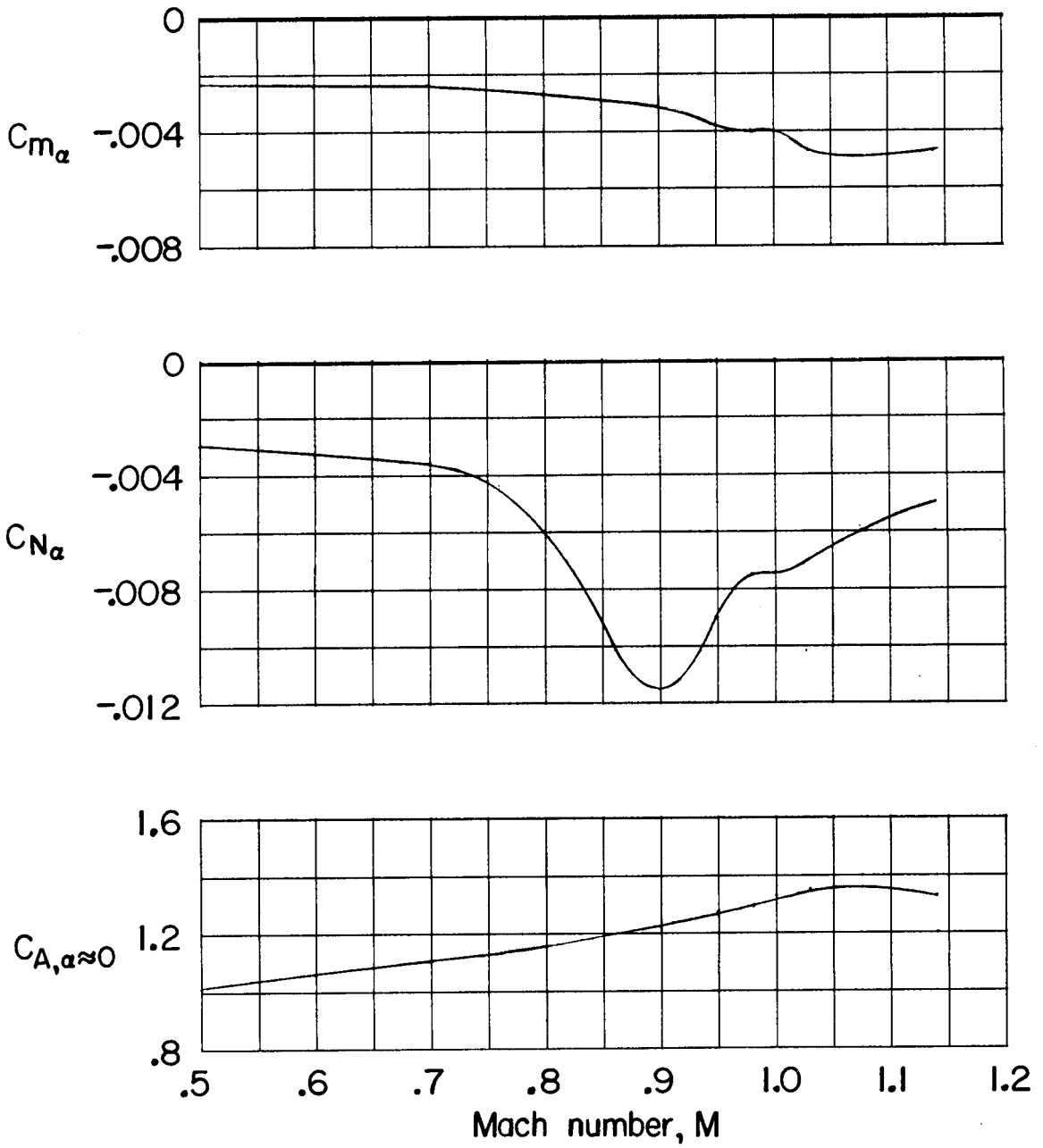

(b) Reentry configuration.

Figure 8.- Continued.

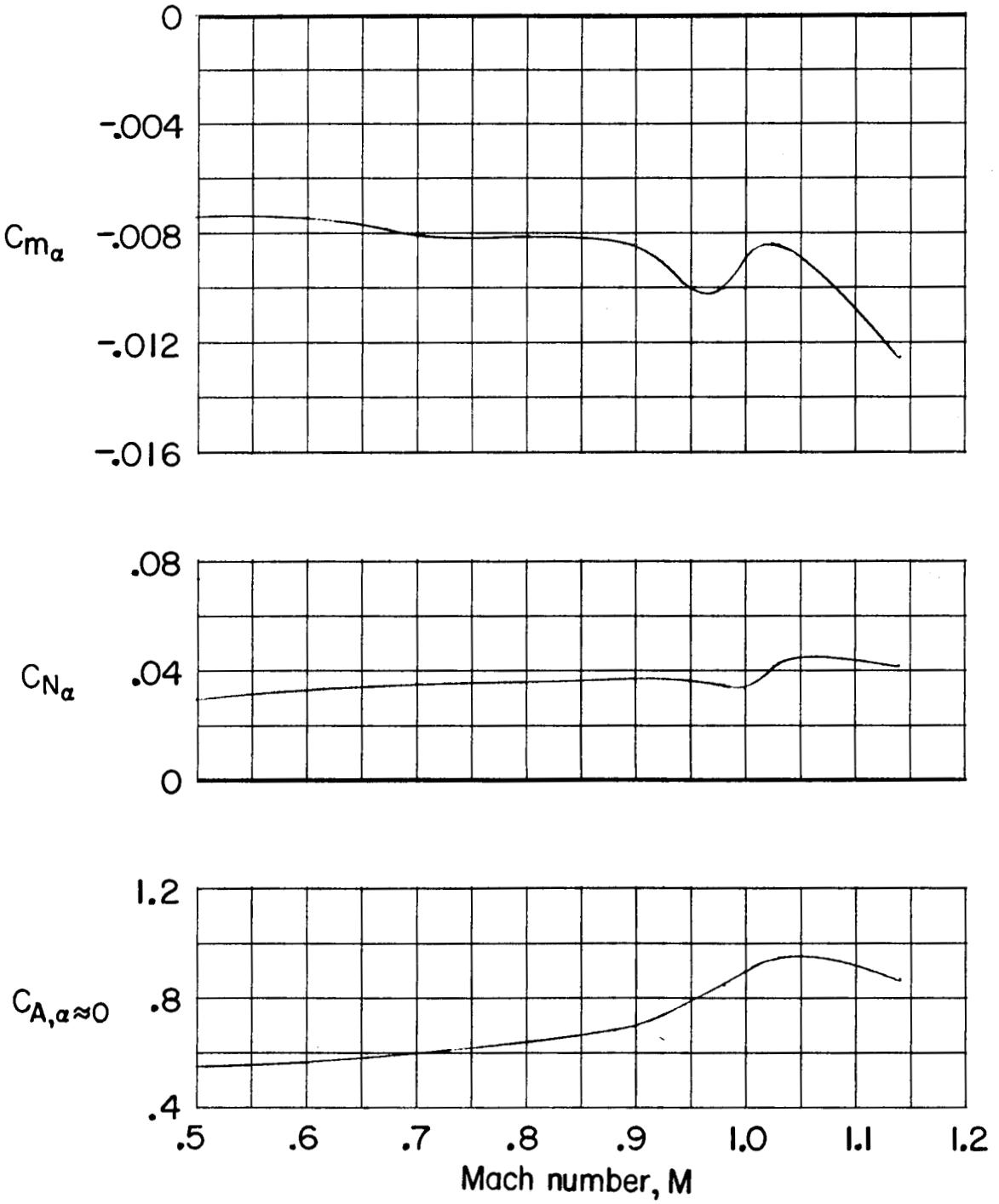

(c) Escape configuration.

Figure 8.- Concluded.

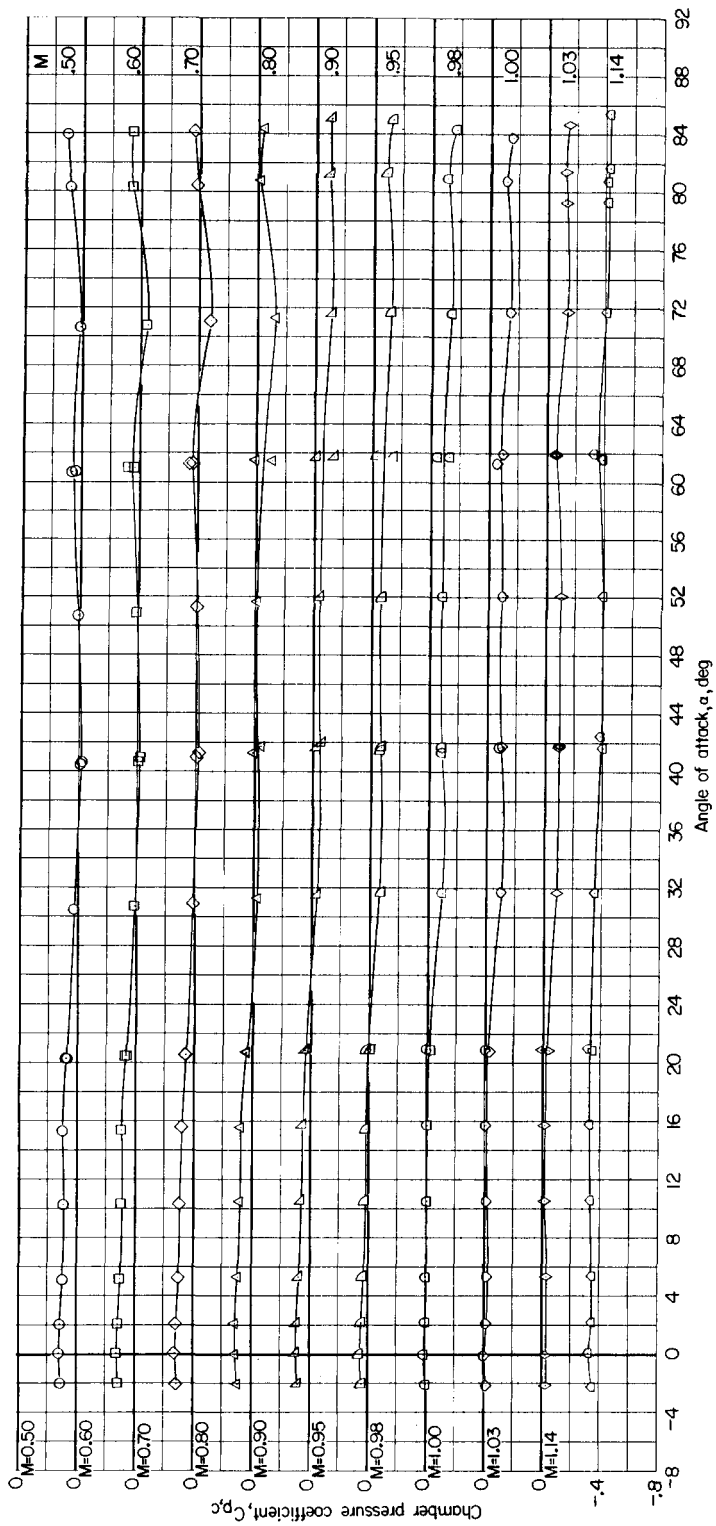

(a) Exit configuration.

Figure 9.- Variation of model chamber-pressure coefficient with angle of attack.

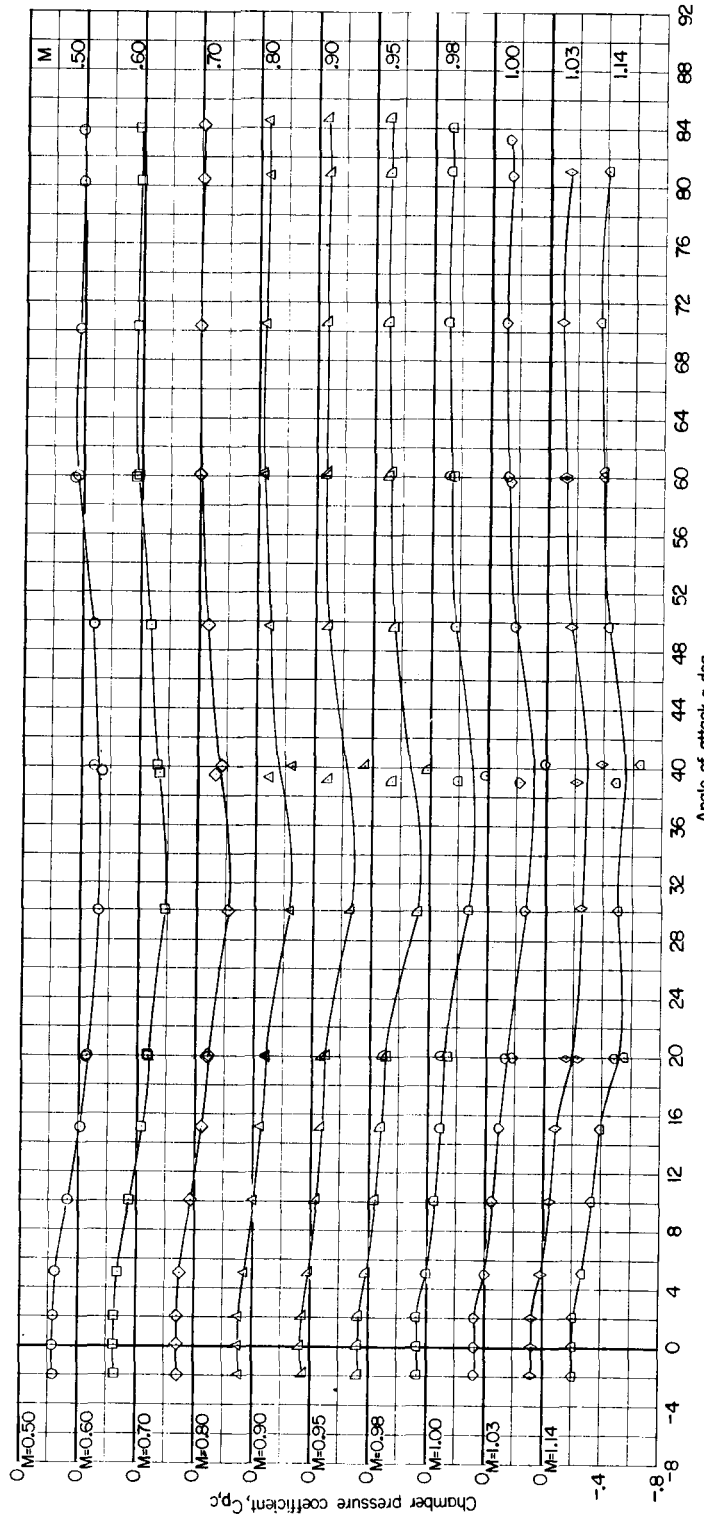

(b) Reentry configuration.

Figure 9.- Continued.

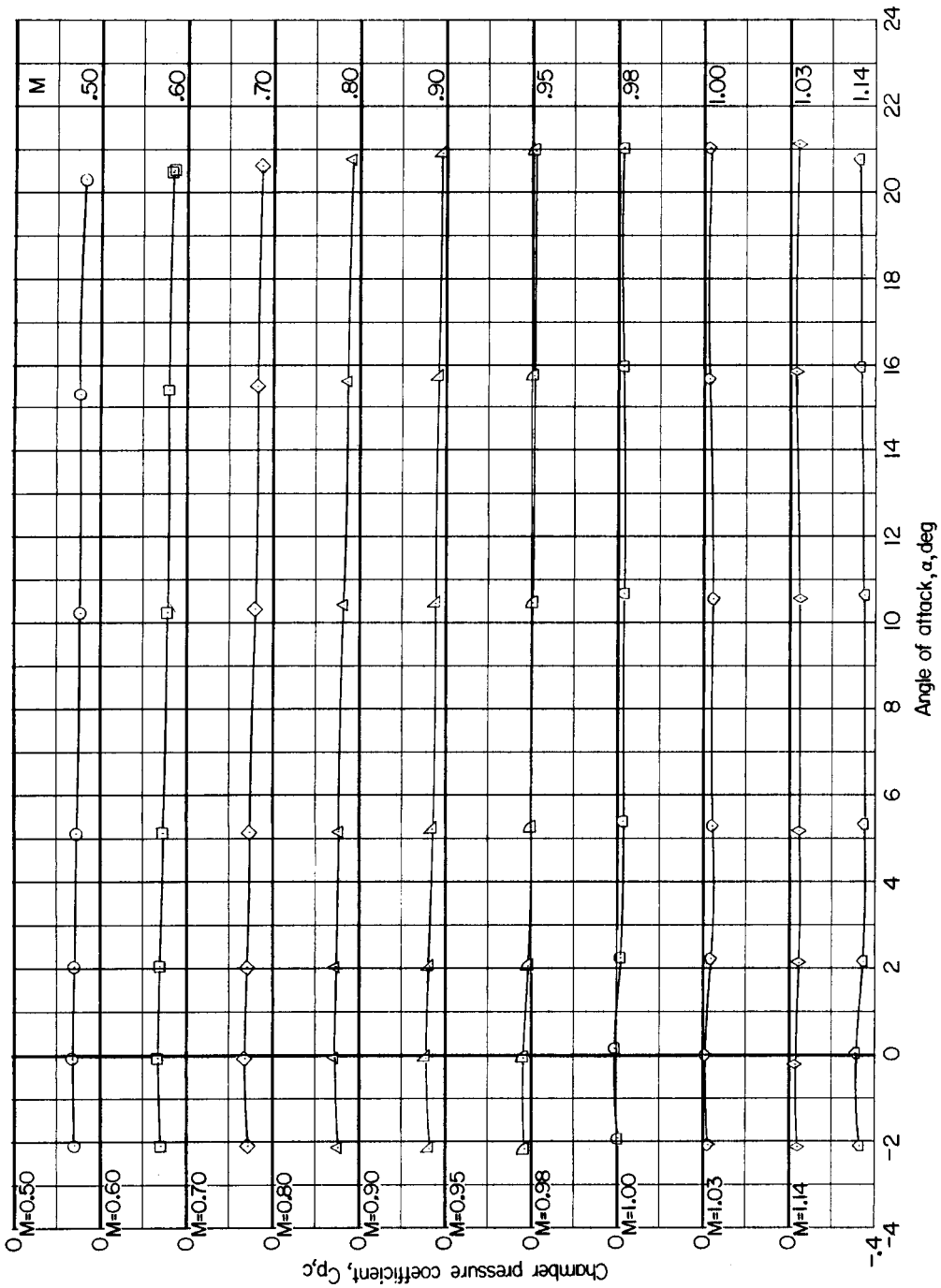

(c) Escape configuration.

Figure 9.- Concluded.